arXiv:1407.4901v2 [gr-qc] 23 Aug 2014

Black hole quasinormal modes in a scalar-tensor theory with field derivative coupling to the Einstein tensor

Masato Minamitsuji[1]

[1]*Multidisciplinary Center for Astrophysics (CENTRA), Instituto Superior Técnico, Lisbon 1049-001, Portugal.*

(Dated: August 26, 2014)

We investigate the quasinormal modes of a test massless, minimally coupled scalar field on a static and spherically symmetric black hole in the scalar-tensor theory with field derivative coupling to the Einstein tensor, which is a part of the Horndeski theory with the shift symmetry. In our solution, the spacetime is asymptotically AdS (anti-de Sitter), where the effective AdS curvature scale is determined solely by the derivative coupling constant. The metric approaches the AdS spacetime in the asymptotic infinity limit and precisely recovers the Schwarzschild-AdS solution in general relativity if the coupling constant is tuned to the inverse of the cosmological constant. We numerically find the lowest lying quasinormal frequency for the perturbation about a test massless, minimally coupled scalar field. The quasinormal frequency agrees with that of the Schwarzschild-AdS solution for the tuned case. For other parameters, in the large black hole limit, as the metric coincides with that of the Schwarzschild-AdS black hole, the quasinormal frequency almost agrees with that of the Schwarzschild-AdS black hole and is insensitive to the value of the cosmological constant. On the other hand, for a small back hole the real part of the quasinormal frequency decreases as the absolute value of the cosmological constant increases.

PACS numbers: 04.50.Kd,04.70.Bw
Keywords: Modified theories of gravity, Classical black holes, Quasinormal Modes.

I. INTRODUCTION

Possible modifications of Einstein's general relativity on cosmological scales have been explored as the alternatives to the Concordance Model of cosmology [1]. A naive modification of general relativity provides ghost degrees of freedom arising from the higher derivative terms as well as inconsistencies with tests of general relativity. In order to avoid the appearance of the ghost degrees, the equations of motion should be of the second order. On the other hand, in order to pass tests of general relativity, a realistic modification of gravity should contain a mechanism to suppress scalar interactions on small scales [2]. After the investigations of a number of models, it has turned out that successful models of the modified gravity can be rewritten in the form of the most general scalar-tensor theory. Such a theory was already proposed by Hordenski [3] forty years ago, and has been reformulated with the growing interest in the various cosmological problems [4]. Despite the existence of the various derivative interactions, in the Horndeski theory the equations of motion remain of the second order [3, 4]. So far, the Horndeski theory has been mainly applied to the cosmological problems.

There has also been the growing interest in the stationary solutions in this theory. So far, for the particular class of the Horndeski theory with the shift symmetry, the static, spherically symmetric black hole solutions have been derived in Refs. [5–8]. These works have considered the theory where the first order derivative of the scalar field is nonminimally coupled to the Einstein tensor

$$S = \frac{1}{2}\int d^4x\sqrt{-g}\Big[m_p^2(R-2\Lambda) - \big(g^{\mu\nu}-\frac{z}{m_p^2}G^{\mu\nu}\big)\partial_\mu\phi\partial_\nu\phi\Big], \quad (1)$$

where $g_{\mu\nu}$ is the metric, $g=\det(g_{\mu\nu})$, R and $G_{\mu\nu}$ are the Ricci scalar and the Einstein tensor associated with the metric $g_{\mu\nu}$, respectively, the dimensionless parameter z characterizes the strength of the field derivative coupling to the Einstein tensor, Λ is the cosmological constant, and m_p is the reduced Planck mass. Clearly, the theory (1) is invariant under the shift transformation $\phi\to\phi+$const. Under the assumption that the scalar field is a C^0 function of the radial coordinate, whose derivatives diverge at the horizon [1], the static black hole solutions have been obtained in [5–9]. These solutions are asymptotically AdS (anti-de Sitter) [5–8] and asymptotically Lifshitz [9], respectively [2]. On the other hand, in [6], it was found that in case that there is the linear time dependence to the scalar field, the theory (1) contains the stealth black hole solution where the scalar field does not backreact on the metric and hence the spacetime remains that of Schwarzschild black hole in general relativity (see also [9]). More recently, these solutions have

[1] The coordinate invariants constructed from the scalar field are regular in the whole spacetime including the horizon.

[2] See also [10] for a no-hair argument for an asymptotically flat solution in this class of scalar-tensor theory without cosmological constant.

been extended to the case of the more general classes of the Horndeski theory [11, 12].

The purpose of this paper is to investigate the quasinormal modes of a test massless, minimally coupled scalar field in the black hole background in the theory (1). The black hole solutions found in the theory (1) are asymptotically AdS. Thus properties of the quasinormal modes in our model would have much overlap with those of the asymptotically AdS black hole solutions found previously. The first study of the quasinormal ringing for conformally coupled scalar waves in AdS was performed by Chan and Mann [16]. Horowitz and Hubeny [15] have investigated quasinormal frequency of a test massless, minimally coupled scalar field on the background of the Schwarzschild-AdS black hole. For a large AdS black hole, both the real and imaginary parts of the quasinormal frequency scale linearly with the black hole temperature, but for a small AdS black hole they deviate from the proportionality relation. The analyses about the Schwarzschild-AdS black hole, including a small AdS black hole, have been followed by Refs. [17, 18]. Then the analysis of quasinormal modes in the asymptotically AdS black hole solutions have been extended to the various cases: AdS black holes with other kinds of horizon topology [19], perturbations about the other fields [20], Reissner-Nortström-AdS black holes [21], Kerr(-Newman)-AdS black holes [22] and BTZ (Bañados-Teitelboim-Zanelli) black holes [23] (for more recent studies, see [24] and references therein). The search of the quasinormal frequency for the asymptotically AdS black holes has also been activated by the growing interests in the AdS/CFT (anti-de Sitter/conformal field theory) correspondence [13]. According to the AdS/CFT correspondence, a black hole in AdS corresponds to a thermal state in the CFT, and the decay of a test field in the AdS black hole spacetime corresponds to the decay of the perturbed CFT state. The quasinormal frequencies correspond to the poles of the retarded correlation function in the dual CFT [14], and the imaginary part of the quasinormal frequency determines the relaxation time scale back to the thermal equilibrium [15]. Thus the analysis of the quasinormal modes in our model may also provide us a hint for the quantum field theory dual to the scalar-tensor theory (1) and also a more general class of the Horndeski theory, which has not been much explored yet.

The construction of this paper is as follows: In Sec. II, we review the black hole solutions in our model. In Sec. III, we discuss the general behavior of a massless, minimally coupled scalar field on top of the black hole background. In Sec. IV, we numerically investigate the quasinormal frequency and discuss their properties. The last Sec. V is devoted to giving the brief summary and conclusion.

II. BLACK HOLE SOLUTIONS

Now, let us review the background black hole solution considered in this paper. In the case of the positive coupling constant $z > 0$, a static and spherically symmetric black hole solution is given by

$$ds^2 = -f(r)dt^2 + g(r)dr^2 + r^2 d\Omega^2, \quad \phi = \phi(r), \qquad (2)$$

where

$$\begin{aligned} f(r) &= \frac{m_p^3}{3rz(m_p^2-\Lambda z)^2}\Big\{ -24mz + m_p^3 r^3\Big(1-\frac{\Lambda z}{m_p^2}\Big)^2 \\ &- 3m_p rz\Big(-1+\frac{\Lambda z}{m_p^2}\Big)\Big(3+\frac{\Lambda z}{m_p^2}\Big) \\ &+ 3z^{3/2}\Big(1+\frac{\Lambda z}{m_p^2}\Big)^2 \arctan\Big(\frac{m_p r}{\sqrt{z}}\Big)\Big\}, \\ g(r) &= \frac{m_p^4\big(2z+r^2(m_p^2-\Lambda z)\big)^2}{(m_p^2 r^2+z)^2(m_p^2-\Lambda z)^2 f(r)}, \\ (\phi'(r))^2 &= -\frac{m_p^8 r^2(m_p^2+\Lambda z)\big(2z+r^2(m_p^2-\Lambda z)\big)^2}{(m_p^2 r^2+z)^3(m_p^2-\Lambda z)^2 z f(r)}, \end{aligned} \qquad (3)$$

the domain of the radial coordinate r is given by $0 < r < \infty$, $d\Omega^2$ represents the line element of a unit two-sphere and the prime represents the derivative with respect to r. The solution without a cosmological constant $\Lambda = 0$ was obtained in [5], which was then generalized to the case for a nonzero cosmological constant $\Lambda \neq 0$ in [6–8]. As we mentioned previously, the asymptotic structure of the spacetime in the large r limit becomes AdS, irrespective of the sign of the cosmological constant. This can be seen by taking the large-r limit;

$$\begin{aligned} f(r) &= \frac{m_p^2}{3z}r^2 + \frac{3m_p^2+\Lambda z}{m_p^2-\Lambda z} + O(r^{-1}), \\ \frac{1}{g(r)} &= \frac{m_p^2}{3z}r^2 + \frac{7m_p^2+\Lambda z}{3m_p^2-3\Lambda z} + O(r^{-1}), \end{aligned} \qquad (4)$$

which is very similar to the static coordinate of the AdS spacetime. From the leading order r^2 terms, we can read the effective AdS curvature scale $\ell_{\rm eff} := \frac{\sqrt{3z}}{m_p}$, which does not depend on the cosmological constant Λ. As $f(r) = 0$ has only a single root even for a large positive cosmological constant $\Lambda > 0$, the only event horizon can be formed at the place where $f(r) = 0$ and no cosmological horizon exist. Moreover, choosing a too large positive cosmological constant $\Lambda > \frac{m_p^2}{z}$ gives rise to an additional curvature singularity at the finite $r = r_s := \sqrt{\frac{2z}{\Lambda z - m_p^2}}$, where $g(r) = 0$, other than the curvature singularity at the center $r = 0$. Thus in order to circumvent the appearance of such a singularity, we have to impose $\Lambda < \frac{m_p^2}{z}$. Furthermore, in order to obtain healthy behaviors of the spacetime and the scalar field outside the horizon, more precisely for the scalar field not to be ghostlike outside

the horizon and also for the black hole to be thermodynamically well-behaved, for a given coupling constant $z > 0$, we also have to impose

$$-2m_p^2 \leq \Lambda z \leq -m_p^2, \tag{5}$$

which does not allow for a vanishing or positive cosmological constant [8]. When the inequality (5) is saturated on the upper bound $\Lambda z = -m_p^2$, the scalar field becomes trivial and the Schwarzschild-AdS solution is recovered:

$$f(r) = 1 - \frac{2m}{m_p r} - \frac{\Lambda}{3} r^2, \quad g(r) = \frac{1}{f(r)}. \tag{6}$$

As in (4) the leading r^2 terms do not vanish unless the limit of $z \to \infty$ is taken [5], the solution (3) does not contain the asymptotically flat case for the finite coupling constant. In the rest, instead of m, we parametrize the size of the black hole by the horizon position $f(r_h) = 0$, and as for the Schwarzschild-AdS black hole solution, call the black holes with $\frac{r_h}{\ell_{\rm eff}} \gg 1$ and $\frac{r_h}{\ell_{\rm eff}} \ll 1$ the 'large' and 'small' black holes, respectively.

Before proceeding, we explain why we do not consider the case of $z < 0$. For $z < 0$, the very similar static solution can be obtained [5, 7, 8] as

$$\begin{aligned} f(r) \;=\; & \frac{m_p^3}{3rz(m_p^2 - \Lambda z)^2}\Big\{ -24mz + m_p^3 r^3 \Big(1 - \frac{\Lambda z}{m_p^2}\Big)^2 \\ & -\; 3m_p rz\Big(-1 + \frac{\Lambda z}{m_p^2}\Big)\Big(3 + \frac{\Lambda z}{m_p^2}\Big) \\ & +\; 3z(-z)^{1/2}\Big(1 + \frac{\Lambda z}{m_p^2}\Big)^2 \operatorname{arctanh}\Big(\frac{m_p r}{\sqrt{-z}}\Big)\Big\}, \end{aligned} \tag{7}$$

where $g(r)$ and $(\phi'(r))^2$ remain the same as (3). The difference from the case of $z > 0$ is that the radial coordinate has the finite domain $0 < r < \frac{\sqrt{-z}}{m_p}$. In this case, in order to realize $(\phi')^2 > 0$ outside the horizon, we have to impose $\Lambda > \frac{m_p^2}{|z|}$. But at the same time an additional curvature singularity appears at the finite radius $r = r_s = \sqrt{\frac{2|z|}{m_p^2 + \Lambda|z|}} (< \frac{\sqrt{|z|}}{m_p})$ which may not be hidden by the horizon [8]. For $\Lambda > \frac{m_p^2}{|z|}$, the weak energy condition for the scalar field is also violated outside the horizon, implying a quantum instability of the solution. Thus in the rest we will focus on the case $z > 0$.

III. MASSLESS SCALAR FIELD PERTURBATIONS

Having introduced the background solution, we consider the general behaviors of a test massless, minimally coupled scalar field obeying the equation of motion $\Box\varphi = 0$, where $\Box$ is the d'Alembertian operator defined in the background given by (2) with (3). We have to emphasize that this test scalar field φ is different from the scalar field ϕ in the original scalar-tensor theory (1). Decomposing the test scalar field into the partial modes

$$\varphi(x^\mu) = \sum_{\ell m} \frac{R(r)}{r} e^{-i\omega t} Y_{\ell m}(\Omega), \tag{8}$$

where $R(r)$ is the radial mode function, $Y_{\ell m}(\Omega)$ is the spherical harmonics on the unit two-sphere S^2, ℓ and m are the angular and magnetic quantum numbers, and ω is the frequency. Introducing the tortoise coordinate $dr_* = \sqrt{\frac{g}{f}} dr$, the radial equation is given by

$$\Big[-\frac{d^2}{dr_*^2} + V(r)\Big] R(r) = \omega^2 R(r), \tag{9}$$

where the effective potential is given by

$$\begin{aligned} V(r) \;=\; & f(r)\Big[\frac{\ell(\ell+1)}{r^2} + \frac{m_p^2 r^2 + z}{3m_p^5 z\big(m_p^2 r^3 + rz(2 - r^2\Lambda)\big)^3}\Big\{ m_p^{11} r^4 (2r^3 + r_h^3) - 3m_p (r - r_h) z^5 \Lambda^2 (-2 + 3r^2\Lambda) \\ & +\; m_p^7 z^2 \big(25r^3 + 2r_h^3 - 16\Lambda r^5 + 6r^7\Lambda^2 + r^2 r_h (9 - 5r_h^2\Lambda) + 3r^4 r_h \Lambda(-5 + r_h^2\Lambda)\big) \\ & +\; m_p^5 z^3 \big(6r + 18r_h + r^3\Lambda - 4r_h^3\Lambda + 8r^5\Lambda^2 - 2r^7\Lambda^3 + r^4 r_h \Lambda^2 (3 - r_h^2\Lambda) + r^2 r_h \Lambda(-33 + 7r_h^2\Lambda)\big) \\ & +\; m_p^9 r^2 z \big(8r^3 + r_h^3 - 6r^5\Lambda + r^2(9r_h - 3r_h^3\Lambda)\big) \\ & +\; m_p^3 (r - r_h)\Lambda z^4 \big[12 + \Lambda\big(-17r^2 - 2rr_h - 2r_h^2 + 3r^2 r_h (r + r_h)\Lambda\big)\big] \\ & +\; 3z^{\frac{3}{2}} (m_p^2 + \Lambda z)^2 \big(m_p^4 r^4 + z^2(2 - 3r_h^2\Lambda) + m_p^2 z r^2 (1 - r^2\Lambda)\big)\Big(\arctan\Big(\frac{m_p r_h}{\sqrt{z}}\Big) - \arctan\Big(\frac{m_p r}{\sqrt{z}}\Big)\Big)\Big\}\Big]. \end{aligned} \tag{10}$$

In the near horizon limit $r \to r_h$, $r_* \simeq \ln(r - r_h) \to -\infty$. On the other hand, in the asymptotic infinity $r \to +\infty$, $r_* \to 0-$. In the asymptotically AdS spacetime, as in Ref. [15], we define the quasinormal modes so that they satisfy the ingoing boundary condition at the horizon $r_* \to -\infty$ and the regularity condition at the spatial

infinity $r_* \to 0-$. As for the case of the Schwarzschild-AdS black hole, $V(r)$ vanishes at the horizon $r = r_h$, because $f(r_h) = 0$ and the combination inside the square bracket in Eq. (10) is regular there. Outside the horizon, $r > r_h$, $V(r)$ is monotonically increasing as r increases. As the function of r_*, $V(r)$ is exponentially suppressed in the near horizon region $r_* \to -\infty$ and the asymptotic behavior of the mode function is given by $R \simeq D_1 e^{-i\omega r_*} + D_2 e^{i\omega r_*}$. The purely ingoing boundary condition gives $D_2 = 0$. On the other hand, in the asymptotic infinity $R \simeq \frac{E_1}{r^2} + E_2 r$. The regularity at the infinity gives $E_2 = 0$. As there is no analytic solution of (9) with (10), we need to search the quasinormal frequency numerically. The details of our method for the numerical search of the quasinormal frequency will be explained later.

When we numerically integrate the equation of motion, it is convenient to redefine the mode function by separating the ingoing mode function at the horizon from the whole radial mode function by $R(r) = e^{-i\omega r_*}\tilde{R}(r)$, where $\tilde{R}(r)$ satisfies the boundary conditions at the horizon $r = r_h$ and at the infinity $r \to \infty$, $\tilde{R}(r_h) = 1$ and $\tilde{R}(\infty) = 0$, respectively. The radial equation of motion (9) then reduces to the form of

$$\tilde{R}'' + \Big\{\Big(\frac{f'}{2f} - \frac{g'}{2g}\Big) - 2i\omega\Big(\frac{g}{f}\Big)^{\frac{1}{2}}\Big\}\tilde{R}' + \Big\{-\frac{\ell(\ell+1)}{r^2}g + \frac{1}{2r}\Big(\frac{g'}{g} - \frac{f'}{f}\Big)\Big\}\tilde{R} = 0. \quad (11)$$

Following [15], we firstly confirm that the imaginary part of an eigenvalue ω is always nonpositive. Multiplying $\big(\frac{f}{g}\big)^{\frac{1}{2}}$ on (11), we find

$$\frac{d}{dr}\Big[\Big(\frac{f}{g}\Big)^{\frac{1}{2}}\tilde{R}'\Big] - 2i\omega\tilde{R}' + \Big(\frac{f}{g}\Big)^{\frac{1}{2}}\Big\{-\frac{\ell(\ell+1)}{r^2}g + \frac{1}{2r}\Big(\frac{g'}{g} - \frac{f'}{f}\Big)\Big\}\tilde{R} = 0. \quad (12)$$

Then, multiplying $\tilde{R}^*$ and integrating by parts with the use of the boundary conditions, $\tilde{R}(\infty) \to 0$ and $(f/g)|_{r\to r_h} \to 0$, we find

$$\int_{r_h}^{\infty} dr\Big\{\Big(\frac{f}{g}\Big)^{\frac{1}{2}}\Big|\tilde{R}'\Big|^2 + 2i\omega\tilde{R}^*\tilde{R}' + \Big(\frac{f}{g}\Big)^{\frac{1}{2}}\Big[\frac{\ell(\ell+1)}{r^2}g + \frac{1}{2r}\Big(\frac{f'}{f} - \frac{g'}{g}\Big)\Big]|\tilde{R}|^2\Big\} = 0. \quad (13)$$

Both the real and imaginary parts of the above equation must vanish separately. The imaginary part of (13) is given by

$$0 = \int_{r_h}^{\infty} dr\Big[\omega\tilde{R}^*\tilde{R}' + \omega^*(\tilde{R}^*)'\tilde{R}\Big] = (\omega - \omega^*)\int_{r_h}^{\infty} dr\tilde{R}^*\tilde{R}' - \omega^*|\tilde{R}(r_h)|^2, \quad (14)$$

where we have used the regularity at the infinity, $\tilde{R}(\infty) = 0$, and hence

$$2i\mathrm{Im}(\omega)\int_{r_h}^{\infty} dr\tilde{R}^*\tilde{R}' = \omega^*\big|\tilde{R}(r_h)\big|^2. \quad (15)$$

Substituting (15) into (13), we obtain

$$\int_{r_h}^{\infty} dr\Big(\frac{f}{g}\Big)^{\frac{1}{2}}\Big\{\Big|\tilde{R}'\Big|^2 + \Big[\frac{\ell(\ell+1)}{r^2}g + \frac{1}{2r}\Big(\frac{f'}{f} - \frac{g'}{g}\Big)\Big]|\tilde{R}|^2\Big\} = -\frac{|\omega|^2}{\mathrm{Im}(\omega)}\big|\tilde{R}(r_h)\big|^2. \quad (16)$$

Since in our background $\frac{\ell(\ell+1)}{r^2}g + \frac{1}{2r}\Big(\frac{f'}{f} - \frac{g'}{g}\Big)$ is positive and regular outside the horizon $r > r_h$, the left-hand side of (16) is positive definite. Thus in order for the right-hand side to be also positive definite, we have to impose $\mathrm{Im}(\omega) < 0$, meaning that the eigenmodes are always decaying.

Following the arguments in [15], as for the Schwarzschild-AdS black holes in general relativity, we also expect the scaling properties of the quasinormal frequency for a large black hole $\frac{r_h}{\ell_{\rm eff}} \gg 1$. Introducing the dimensionless coordinate $y := \frac{r}{r_h}$ to fix the horizon at $y = 1$, for the large black hole the metric can be approximated as

$$ds^2 \simeq -\Big(-\frac{1}{y} + y^2\Big)\frac{r_h^2}{\ell_{\rm eff}^2}dt^2 + \frac{\ell_{\rm eff}^2 y}{(-1+y^3)}dy^2 + r_h^2 y^2 dx_i dx^i, \quad (17)$$

Thus the metric in this limit is invariant under the rescaling of $t \to at$, $x^i \to ax^i$ and $r_h \to \frac{r_h}{a}$, where a is a constant. The time-dependent part of the quasinormal mode function, $e^{-i\omega t}$, is invariant under the above rescaling, which results in the rescaling of the frequency as $\omega \to \frac{\omega}{a}$. Thus, as both r_h and ω have the same scaling property, the quasinormal frequency for a large black hole should scale linearly with the horizon radius, $\omega \propto r_h$. As argued in [8], the temperature of the black hole is explicitly given by $T = \frac{m_p^2(m_p^2 r_h^2 + z(2-\Lambda r_h^2))}{4\pi r_h z(m_p^2 - \Lambda z)}$, which behaves as that of the Schwarzschild-AdS black hole [25]. For a large black hole, the temperature scales as $T = \frac{m_p^2 r_h}{4\pi z}$, and hence the quasinormal frequency will also linearly scale with the temperature [15]. In addition, the limiting behavior (17) does not depend on the cosmological constant Λ and agrees with the large black hole limit of the Schwarzschild-AdS spacetime with the curvature scale $\ell_{\rm eff}$. Thus for a large black hole, the quasinormal frequency should not be sensitive to the value of Λ.

IV. QUASINORMAL MODES

We then numerically confirm the quasinormal frequency. Introducing the new dimensionless coordinate

$x := \frac{r_h}{r} (= y^{-1})$, the radial equation (11) can be rewritten as

$$S(x)\frac{d^2}{dx^2}\tilde{R} + T(x,\omega)\frac{d}{dx}\tilde{R} + U(x)\tilde{R} = 0, \qquad (18)$$

where

$$\begin{aligned} S(x) &:= -x^4\Big(\frac{f}{g}\Big)^{\frac{1}{2}}, \\ T(x,\omega) &:= -x^4\Big\{\Big(\frac{f}{g}\Big)^{\frac{1}{2}}\Big(\frac{2}{x} + \frac{f_x}{2f} - \frac{g_x}{2g}\Big) + \frac{2i\omega r_h}{x^2}\Big\}, \\ U(x) &= \Big(\frac{f}{g}\Big)^{\frac{1}{2}}\Big\{\ell(\ell+1)x^2 g + \frac{x^3}{2}\Big(\frac{g_x}{g} - \frac{f_x}{f}\Big)\Big\}. \end{aligned} \qquad (19)$$

There are two regular singular points in Eq. (18); $x = 0$ (the infinity) and $x = 1$ (the horizon). We then derive the boundary conditions. By taking the limit to the horizon $x \to 1$ with the assumption that $\frac{d^2\tilde{R}}{dx^2}$ is smooth, the boundary condition on the horizon is given by $\tilde{R}(1) = 1$ and $\frac{d}{dx}\tilde{R}\Big|_{x=1} = -\frac{U(1)}{T(1,\omega)}$. On the other hand, the boundary condition at the asymptotic infinity is given by the regularity condition $\tilde{R}(0) = 0$.

For the numerical search, we fix $m_p = 1$. Thus the quantities in all the tables and in all the axes of figures in this paper are measured in the unit of $m_p = 1$. Note also that the coupling constant z is dimensionless. Our method to search the quasinormal frequency is as follows. For a given set of the parameters, we first consider a trial frequency ω_1 and numerically integrate the equation (18) from the horizon $x = 1$ to the spatial infinity $x = 0$, with the 'initial' conditions at the horizon $\tilde{R}_1(1) = 1$ and $\frac{d}{dx}\tilde{R}_1\Big|_{x=1} = -\frac{U(1)}{T(1,\omega_1)}$. If ω_1 is not the correct eigenvalue ω, the numerical solution $\tilde{R}_1(x)$ fails to satisfy the boundary condition at the infinity, $\tilde{R}_1(0) \neq 0$. We then choose another value of the frequency ω_2 close to ω_1, numerically integrate (18) with the modified 'initial' conditions at the horizon $\tilde{R}_2(1) = 1$ and $\frac{d}{dx}\tilde{R}_2\Big|_{x=1} = -\frac{U(1)}{T(1,\omega_2)}$, and obtain the corresponding numerical solution $\tilde{R}_2(x)$. Although $\tilde{R}_2(x)$ would again fail to satisfy the boundary condition for the quasinormal mode at the spatial infinity, $\tilde{R}_2(0) \neq 0$, the behavior of $\tilde{R}_2(x)$ around $x = 0$ would also be closer to that of the correct quasinormal eigenfunction $\tilde{R}(x)$, with the correct eigenvalue ω and $\tilde{R}(0) = 0$, than that of the first one $\tilde{R}_1(x)$. In this way, we iterate the numerical integration with the new trial frequencies $\omega_3, \omega_4, \omega_5, \cdots$. As the number of iteration k becomes sufficiently large, the behavior of the integrated solution $\tilde{R}_k(x)$ around $x = 0$ is improved very much and the trial value ω_k can be much closer to the correct quasinormal frequency ω. For each set of the parameters, we iterate the numerical integration until the precision higher than values shown in [15, 18] is achieved, as we use values in [15, 18] as the reference (see below). As the Schwarzschild-AdS solution is recovered for $z = -\frac{1}{\Lambda}$, we will make use of the case of $z = \frac{1}{3}$ and $\Lambda = -3$ as the reference solution which gives the unit effective curvature scale $\ell_{\rm eff} = \frac{\sqrt{3z}}{m_p} = 1$ in the unit of $m_p = 1$. Thus as the consistency check, we have confirmed that in the case of $z = \frac{1}{3}$ and $\Lambda = -3$ our method correctly reproduces the quasinormal frequency obtained in Refs. [15, 18] both for the large and small Schwarzschild-AdS black holes.

For each horizon size r_h and angular quantum number ℓ, there is an infinite number of the quasinormal frequencies labeled by the overtone number $n = 0, 1, 2, \cdots$. We often order them in terms of the increasing imaginary part of the quasinormal frequency. The fundamental quasinormal frequency is defind as the one with the lowest imaginary part and labeled by $n = 0$. Similarly, the first overtone has the second lowest imaginary part and labeled by $n = 1$, and so on. Also, the lowest value of the imaginary part corresponds to the lowest value of the real part, the second lowest value of the imaginary part corresponds to the second lowest value of the real part, and so on. Thus the increasing overtone number n also corresponds to the increasing energy of the mode. In this paper, we will present the numerical results for the less damped, lowest lying ($n = 0$) and spherical symmetric ($\ell = 0$) modes, for the various choice of the horizon size r_h. We then will comment on the high overtone ($n \geq 1$) and non-spherically symmetric ($\ell \geq 1$) modes, which are damped more rapidly.

The fundamental quasinormal frequency for $\ell = 0$ in the Schwarzschild-AdS spacetime has been numerically investigated in [15] and subsequent works [17, 18]. Varying either the coupling constant z or the cosmological constant Λ, we investigate how the quasinormal frequency ω scales with these parameters. Within the bounds (5), we consider the following cases

Case 1): fixing $\Lambda = -3$, $\frac{1}{3} \leq z \leq \frac{2}{3}$,

Case 2): fixing $z = \frac{1}{3}$, $3 \leq |\Lambda| \leq 6$.

First, we consider Case 1). In Case 1), as one increases z, the effective AdS curvature scale also increases as $\ell_{\rm eff} = \sqrt{3z}$ in the unit of $m_p = 1$. In Table I, for the various choice of the horizon size r_h, the real and imaginary parts of the quasinormal frequency $\omega = \omega_r - i\omega_i$ are shown, where ω_r and ω_i are real and positive. In Figs. 1-2, they are plotted as the functions of r_h. We find that the behavior of the quasinormal frequency is similar to that of the case of the Schwarzschild-AdS black hole. As the coupling constant z increases, the values of the quasinormal frequency decrease. For $z = \frac{1}{3}$, ω approaches 3, corresponding to the lowest lying normal mode of the AdS spacetime [26]. For a large black hole, we have numerically confirmed that both ω_r and ω_i are proportional to r_h. The proportionality coefficients $\omega_r \approx a_r(z) r_h$ and $\omega_i \approx a_i(z) r_h$ are listed in Table II, and

$$a_r(z) \approx \frac{0.618}{z} \approx \frac{1.85}{\ell_{\rm eff}^2}, \quad a_i(z) \approx \frac{0.888}{z} \approx \frac{2.66}{\ell_{\rm eff}^2}, \qquad (20)$$

This almost agrees with the results shown in Ref. [15] and is consistent with our previous arguments. Namely,

TABLE I: Quasinormal frequency ω for $\Lambda = -3$. Note that the quantities in the table are measured in the unit of $m_p = 1$.

r_h	0.01		0.03		0.05	
z	ω_r	ω_i	ω_r	ω_i	ω_r	ω_i
$\frac{1}{3}$	2.9738	0.00054711	2.9167	0.0058571	2.8539	0.019329
0.40	2.5423	0.00042496	2.4967	0.0044909	2.4468	0.014671
0.50	2.0831	0.00031269	2.0488	0.0032583	2.0155	0.010520
0.60	1.7603	0.00024380	1.7331	0.0025147	1.7033	0.0080482
$\frac{2}{3}$	1.5937	0.00021128	1.5699	0.0021677	1.5439	0.0069039
r_h	0.07		0.10		0.30	
z	ω_r	ω_i	ω_r	ω_i	ω_r	ω_i
$\frac{1}{3}$	2.7882	0.043587	2.6928	0.10096	2.3845	0.70413
0.40	2.3943	0.032959	2.3169	0.076727	2.0532	0.56339
0.50	1.9715	0.023504	1.9121	0.054899	1.6975	0.42695
0.60	1.6719	0.017892	1.6244	0.041829	1.4445	0.33931
$\frac{2}{3}$	1.5165	0.015305	1.4748	0.035776	1.3136	0.29680
r_h	0.50		0.70		1.0	
z	ω_r	ω_i	ω_r	ω_i	ω_r	ω_i
$\frac{1}{3}$	2.3830	1.2972	2.5014	1.8569	2.7982	2.6712
0.40	2.0451	1.0540	2.1386	1.5192	2.3793	2.1981
0.50	1.6855	0.81377	1.7562	1.1831	1.9437	1.7248
0.60	1.4320	0.65650	1.4888	0.96119	1.6425	1.4101
$\frac{2}{3}$	1.3008	0.57913	1.3510	0.85131	1.4882	1.2536
r_h	3.0		5.0		7.0	
z	ω_r	ω_i	ω_r	ω_i	ω_r	ω_i
$\frac{1}{3}$	5.9158	8.0012	9.4711	13.3255	13.1066	18.6517
0.40	4.9527	6.6514	7.9070	11.0941	10.9326	15.5355
0.50	3.9823	5.2989	6.3384	8.8607	8.7554	12.4177
0.60	3.3303	4.3955	5.2895	7.3704	7.3016	10.3380
$\frac{2}{3}$	3.0025	3.9434	4.7639	6.6246	6.5638	9.2978
r_h	10		20		50	
z	ω_r	ω_i	ω_r	ω_i	ω_r	ω_i
$\frac{1}{3}$	18.6070	26.6418	37.0449	53.2787	92.4937	133.1933
0.40	15.5132	22.1961	30.8745	44.3962	77.0795	110.9940
0.50	12.4171	17.7497	24.7028	35.5131	61.6649	88.7931
0.60	10.3514	14.7841	20.5876	29.5906	51.3882	73.9928
$\frac{2}{3}$	9.3180	13.3010	18.5297	26.6292	46.2497	66.5922

TABLE II: $a_r(z)$ an $a_i(z)$ for $\Lambda = -3$. Note that the quantities in the table are measured in the unit of $m_p = 1$.

z	a_r	a_i
$\frac{1}{3}$	1.8520	2.6639
0.40	1.5435	2.2198
0.50	1.2349	1.7757
0.60	1.0292	1.4796
$\frac{2}{3}$	0.9263	1.3315

as the metric in the large black hole limit (17) agrees with that of the Schwarzschild-AdS spacetime with the effective AdS scale $\ell_{\rm ell}$, ω for a large black hole also coincides with that of the given Schwarzschild-AdS spacetime.

In order to investigate the dependence on the cosmological constant Λ, we then consider Case 2). As in this case $\ell_{\rm eff} = 1$ for any value of Λ, the deviation from the exact Schwarzschild-AdS black holes would be able to be made more explicit. In Table III, ω_r and ω_i are shown for the various choice of the horizon size r_h.

In Figs. 3-4, they are plotted as the functions of r_h. Both ω_r and ω_i decrease as $|\Lambda|$ increases. For a large black hole, however, as all curves are degenerate, the dependence of ω on Λ becomes very week, which was already expected from our argument below (17). In addition, for a large black hole, both ω_r and ω_i

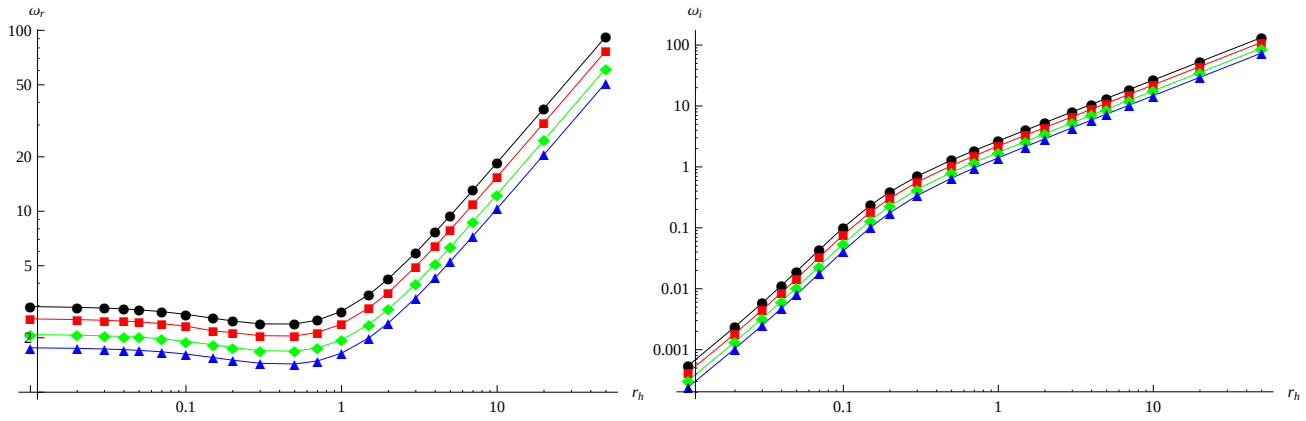

FIG. 1: ω_r and ω_i are shown as the functions of r_h: In both panels, the curves from the top to the bottom correspond to $z = \frac{1}{3}$, 0.40, 0.50 and 0.60, respectively. The case of $z = \frac{1}{3}$ corresponds to that of the Schwarzschild-AdS black hole. Note that the quantities in the axes are measured in the unit of $m_p = 1$.

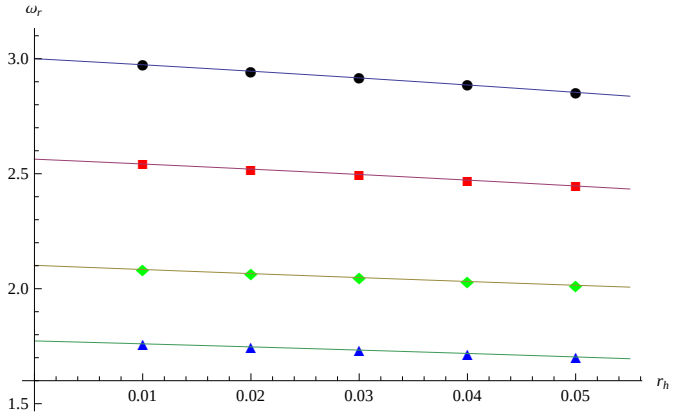

FIG. 2: An enlarged display of ω_r as the function of r_h for small black holes: The curves from the top to the bottom correspond to $z = \frac{1}{3}$, 0.40, 0.50 and 0.60, respectively. The case of $z = \frac{1}{3}$, approaching 3.0 for $r_h \to 0$, corresponds to that of the Schwarzschild-AdS black hole. Note that the quantities in the axes are measured in the unit of $m_p = 1$.

are proportional to r_h. The proportionality coefficients $\omega_r \approx b_r(\Lambda) r_h$ and $\omega_i \approx b_i(\Lambda) r_h$ are listed in Table IV, which are also not sensitive to the value of Λ. On the other hand, for a small black hole ω_r does not exhibit the degenerate behavior as for a large black hole and as $|\Lambda|$ increases the quasinormal frequency decreases.

We then comment on the high overtone ($n \geq 1$) and non-spherically symmetric ($\ell \geq 1$) modes. In the case of the Schwarzschild-AdS spacetime, a complete search of the quasinormal frequency including these highly damped modes was performed in [27]. As argued below (17), in the large black hole limit our black hole spacetime resembles the Schwarzschild-AdS spacetime with $\ell_{\rm eff}$ solely determined by the coupling constant z. Hence, we expect that especially for a large black hole the quasinormal frequency is almost identical to that of the Schwarzschild-AdS spacetime with $\ell_{\rm eff}$ obtained in [27], and also insensitive to the value of Λ. From [27], we expect for the $\ell = 0$ modes, in the large black hole and high overtone limits $(r_h, n) \to \infty$ the quasinormal frequency will behave as

$$\frac{\omega \ell_{\rm eff}^2}{r_h} \approx (1.299 - 2.25i)n + 1.856 - 2.675i, \qquad (21)$$

which is evenly spaced. In addition, from [27] the asymptotic behavior of the spacing of ω, $(1.299 - 2.25i)\frac{r_h}{\ell_{\rm eff}^2}$, is expected to hold also for the any other value of the angular quantum number ℓ, although the offset value for $n = 0$ is ℓ-dependent. On the other hand, for a small black hole we expect more sensitivity to the value of Λ than that for a large black hole, but also an evenly-spaced asymptotic behavior of the quasinormal frequencies in the large n limit, as for the case of the Schwarzschild-AdS black hole [27].

TABLE III: Quasinormal frequency ω for $z = \frac{1}{3}$. Note that the quantities in the table are measured in the unit of $m_p = 1$.

r_h	0.01		0.03		0.05	
Λ	ω_r	ω_i	ω_r	ω_i	ω_r	ω_i
-3	2.9738	0.00054711	2.9167	0.0058571	2.8539	0.019329
-4	2.6713	0.00057213	2.6172	0.0061641	2.5578	0.020393
-5	2.4360	0.00059377	2.3845	0.0064350	2.3277	0.021330
-6	2.2471	0.00061297	2.1977	0.0066798	2.1432	0.022174
r_h	0.07		0.10		0.30	
Λ	ω_r	ω_i	ω_r	ω_i	ω_r	ω_i
-3	2.7882	0.043587	2.6928	0.10096	2.3845	0.70413
-4	2.4960	0.045814	2.4082	0.10469	2.1521	0.69170
-5	2.2693	0.047729	2.1879	0.10952	1.9738	0.68031
-6	2.0876	0.049411	2.0118	0.11020	1.8323	0.66999
r_h	0.50		0.70		1.0	
Λ	ω_r	ω_i	ω_r	ω_i	ω_r	ω_i
-3	2.3830	1.2972	2.5014	1.8569	2.7982	2.6712
-4	2.1847	1.2662	2.3294	1.8157	2.6570	2.6251
-5	2.0334	1.2399	2.1991	1.7819	2.5510	2.5884
-6	1.9142	1.2175	2.0969	1.7538	2.4682	2.5584
r_h	3.0		5.0		7.0	
Λ	ω_r	ω_i	ω_r	ω_i	ω_r	ω_i
-3	5.9158	8.0012	9.4711	13.3255	13.1066	18.6517
-4	5.8579	7.9730	9.4355	13.3075	13.0811	18.6385
-5	5.8175	7.9516	9.4089	13.2939	13.0621	18.6286
-6	5.7808	7.9348	9.3882	13.2832	13.0471	18.6209
r_h	10		20		50	
Λ	ω_r	ω_i	ω_r	ω_i	ω_r	ω_i
-3	18.6070	26.6418	37.0449	53.2787	92.4937	133.1933
-4	18.5891	26.6324	37.0359	53.2740	98.4900	133.1910
-5	18.5756	26.6254	37.0292	53.2705	92.4873	133.1900
-6	18.5652	26.6200	37.0239	52.2677	92.4852	133.1890

TABLE IV: $b_r(\Lambda)$ and $b_i(\Lambda)$ for $z = \frac{1}{3}$. Note that the quantities in the table are measured in the unit of $m_p = 1$.

Λ	b_r	b_i
-3	1.8520	2.6639
-4	1.8516	2.6637
-5	1.8513	2.6636
-6	1.8510	2.6634

V. CONCLUSIONS

Before closing this paper, we will give the brief summary and future prospects. We have numerically investigated the lowest lying quasinormal modes of a test massless, minimally coupled scalar field in a static and spherically black hole background in a class of the Horndeski scalar-tensor theory with field derivative coupling to the Einstein tensor (1), obtained in Refs. [5–8]. We have considered the perturbation about a test massless, minimally coupled scalar field. As our black hole spacetime is asymptotically AdS with the curvature scale $\ell_{\rm eff} = \frac{\sqrt{3z}}{m_p}$, the properties are very similar to those of the Schwarzschild-AdS black holes in general relativity. The metric reproduces that of the Schwarzschild-AdS black hole solution for $\Lambda z = -m_p^2$ where the scalar field becomes trivial. In order to make the solution healthy outside the horizon, we have focused on the range (5) for a fixed coupling constant.

For a fixed Λ, as the coupling constant z increases, both the real and imaginary parts of the quasinormal frequency decrease and scale as $\ell_{\rm eff}^{-2}$. For a fixed coupling constant z, as the metric in the large black hole limit agrees with that of the Schwarzschild-AdS black hole with a fixed $\ell_{\rm eff}$ which does not depend on Λ, the quasinormal frequency in this limit is not sensitive to Λ. For a small black hole, as the metric deviates from that of

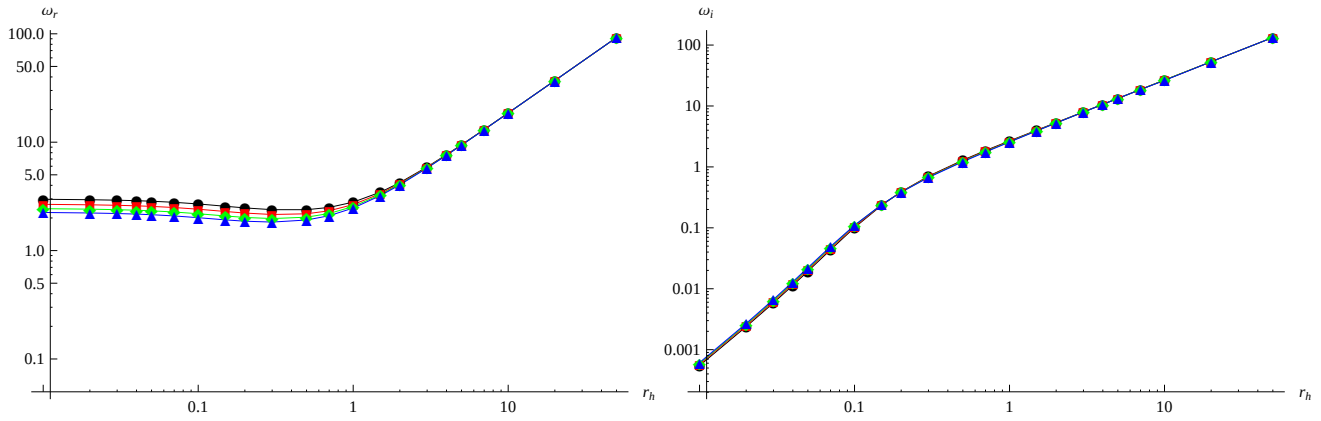

FIG. 3: ω_r and ω_i are shown as the functions of r_h: In the panel of ω_r, the curves from the top to the bottom correspond to $|\Lambda| = 3$, 4, 5 and 6, respectively. The curves of the same type are also used in the panel for ω_i but are almost degenerate. The case of $|\Lambda| = 3$ corresponds to that of the Schwarzschild-AdS black hole. Note that the quantities in the axes are measured in the unit of $m_p = 1$.

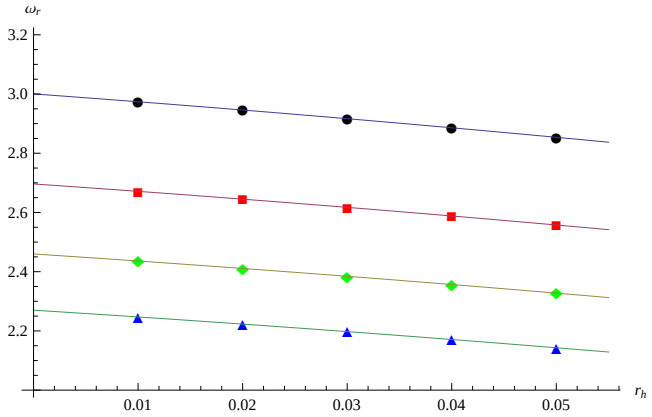

FIG. 4: An enlarged display of ω_r as the function r_h for small black holes: The curves from the top to the bottom correspond to $|\Lambda| = 3$, 4, 5 and 6, respectively. Note that the quantities in the axes are measured in the unit of $m_p = 1$.

the Schwarzschild-AdS spacetime and the dependence of the metric on Λ becomes more explicit, the quasinormal frequency also becomes more sensitive to Λ compared to the case of a large black hole and as $|\Lambda|$ increases ω_r decreases. There would be various extensions of the present analyses, e.g., to include the effects of the mass and couplings of the test scalar field and to investigate the perturbation by another test field with a different spin, especially about the gravitational field, all which may provide us further hints to distinguish two theories more explicitly.

Acknowledgement

This work was supported by the FCT-Portugal through Grant No. SFRH/BPD/88299/2012.

[1] T. Clifton, P. G. Ferreira, A. Padilla and C. Skordis, Phys. Rept. **513**, 1 (2012) [arXiv:1106.2476 [astro-ph.CO]].

[2] A. I. Vainshtein, Phys. Lett. B **39**, 393 (1972); P. Brax, C. van de Bruck, A. -C. Davis, J. Khoury and A. Weltman, Phys. Rev. D **70**, 123518 (2004) [astro-ph/0408415].

[3] G. W. Horndeski, Int. J. Theor. Phys. 10, 363 (1974); C. Deffayet, G. Esposito-Farese and A. Vikman, Phys. Rev. D **79**, 084003 (2009) [arXiv:0901.1314 [hep-th]].

[4] C. Deffayet, S. Deser and G. Esposito-Farese, Phys. Rev. D **80**, 064015 (2009) [arXiv:0906.1967 [gr-qc]]; C. Deffayet, X. Gao, D. A. Steer and G. Zahariade, Phys.

Rev. D **84**, 064039 (2011) [arXiv:1103.3260 [hep-th]]; T. Kobayashi, M. Yamaguchi and J. 'i. Yokoyama, Prog. Theor. Phys. **126**, 511 (2011) [arXiv:1105.5723 [hep-th]].

[5] M. Rinaldi, Phys. Rev. D **86**, 084048 (2012) [arXiv:1208.0103 [gr-qc]].

[6] E. Babichev and C. Charmousis, arXiv:1312.3204 [gr-qc].

[7] A. Anabalon, A. Cisterna and J. Oliva, Phys. Rev. D **89**, 084050 (2014) [arXiv:1312.3597 [gr-qc]].

[8] M. Minamitsuji, Phys. Rev. D **89**, 064017 (2014) [arXiv:1312.3759 [gr-qc]].

[9] M. Bravo-Gaete and M. Hassaine, Phys. Rev. D **89**, 104028 (2014) [arXiv:1312.7736 [hep-th]].

[10] C. Germani, L. Martucci and P. Moyassari, Phys. Rev. D **85**, 103501 (2012) [arXiv:1108.1406 [hep-th]].

[11] C. Charmousis, T. Kolyvaris, E. Papantonopoulos and M. Tsoukalas, arXiv:1404.1024 [gr-qc].

[12] T. Kobayashi and N. Tanahashi, PTEP **2014**, no. 7, 073E02 (2014) [arXiv:1403.4364 [gr-qc]].

[13] J. M. Maldacena, Adv. Theor. Math. Phys. **2**, 231 (1998) [hep-th/9711200]; S. S. Gubser, I. R. Klebanov and A. M. Polyakov, Phys. Lett. B **428**, 105 (1998) [hep-th/9802109]; E. Witten, Adv. Theor. Math. Phys. **2**, 253 (1998) [hep-th/9802150].

[14] D. Birmingham, I. Sachs and S. N. Solodukhin, Phys. Rev. Lett. **88**, 151301 (2002) [hep-th/0112055]; D. T. Son and A. O. Starinets, JHEP **0209**, 042 (2002) [hep-th/0205051]; P. K. Kovtun and A. O. Starinets, Phys. Rev. D **72**, 086009 (2005) [hep-th/0506184].

[15] G. T. Horowitz and V. E. Hubeny, Phys. Rev. D **62**, 024027 (2000) [hep-th/9909056].

[16] J. S. F. Chan and R. B. Mann, Phys. Rev. D **55**, 7546 (1997) [gr-qc/9612026]; J. S. F. Chan and R. B. Mann, Phys. Rev. D **59**, 064025 (1999).

[17] J. -M. Zhu, B. Wang and E. Abdalla, Phys. Rev. D **63**, 124004 (2001) [hep-th/0101133].

[18] R. A. Konoplya, Phys. Rev. D **66**, 044009 (2002) [hep-th/0205142].

[19] B. Wang, E. Abdalla and R. B. Mann, Phys. Rev. D **65**, 084006 (2002) [hep-th/0107243]; R. Aros, C. Martinez, R. Troncoso and J. Zanelli, Phys. Rev. D **67**, 044014 (2003) [hep-th/0211024]; A. S. Miranda and V. T. Zanchin, Phys. Rev. D **73**, 064034 (2006) [gr-qc/0510066]; D. Birmingham and S. Mokhtari, Phys. Rev. D **74**, 084026 (2006) [hep-th/0609028]; A. S. Miranda, J. Morgan and V. T. Zanchin, JHEP **0811**, 030 (2008) [arXiv:0809.0297 [hep-th]].

[20] V. Cardoso and J. P. S. Lemos, Phys. Rev. D **64**, 084017 (2001) [gr-qc/0105103]; S. Musiri and G. Siopsis, Phys. Lett. B **563**, 102 (2003) [hep-th/0301081]; S. Musiri and G. Siopsis, Phys. Lett. B **576**, 309 (2003) [hep-th/0308196]. S. Musiri, S. Ness and G. Siopsis, Phys. Rev. D **73**, 064001 (2006) [hep-th/0511113]; J. J. Friess, S. S. Gubser, G. Michalogiorgakis and S. S. Pufu, JHEP **0704**, 080 (2007) [hep-th/0611005].

[21] B. Wang, C. -Y. Lin and E. Abdalla, Phys. Lett. B **481**, 79 (2000) [hep-th/0003295]; B. Wang, C. Molina and E. Abdalla, Phys. Rev. D **63**, 084001 (2001) [hep-th/0005143]; R. A. Konoplya, Phys. Rev. D **66**, 084007 (2002) [gr-qc/0207028]; E. Berti and K. D. Kokkotas, Phys. Rev. D **67**, 064020 (2003) [gr-qc/0301052]; B. Wang, C. -Y. Lin and C. Molina, Phys. Rev. D **70**, 064025 (2004) [hep-th/0407024]; R. A. Konoplya and A. Zhidenko, Phys. Rev. D **78**, 104017 (2008) [arXiv:0809.2048 [hep-th]]; J. -l. Jing and Q. -y. Pan, Phys. Rev. D **71**, 124011 (2005) [gr-qc/0502011].

[22] E. Winstanley, Phys. Rev. D **64**, 104010 (2001) [gr-qc/0106032]; B. Chen and C. -S. Chu, JHEP **1005**, 004 (2010) [arXiv:1001.3208 [hep-th]]. M. Giammatteo and I. G. Moss, Class. Quant. Grav. **22**, 1803 (2005) [gr-qc/0502046]; S. Dyatlov, Commun. Math. Phys. **306**, 119 (2011) [arXiv:1003.6128 [math.AP]]; S. Yoshida, N. Uchikata, and T. Futamase, Phys. Rev. D, **81**, 044005.

[23] V. Cardoso and J. P. S. Lemos, Phys. Rev. D **63**, 124015 (2001) [gr-qc/0101052]; D. Birmingham, Phys. Rev. D **64**, 064024 (2001) [hep-th/0101194].

[24] E. Berti, V. Cardoso and A. O. Starinets, Class. Quant. Grav. **26**, 163001 (2009) [arXiv:0905.2975 [gr-qc]].

[25] S. W. Hawking and D. N. Page, Commun. Math. Phys. **87**, 577 (1983).

[26] C. P. Burgess and C. A. Lutken, Phys. Lett. B **153**, 137 (1985).

[27] V. Cardoso, R. Konoplya and J. P. S. Lemos, Phys. Rev. D **68**, 044024 (2003) [gr-qc/0305037].